



 Cite this: *RSC Adv.*, 2021, 11, 37063

# Synthesis and the growth mechanism of ultrafine silver nanowires by using 5-chloro-2-thienylmagnesium bromide as the additive†

 Zhengyang Fan, Jie Chen, Huaming Mao, Jungang Yin, Wei Dai, Linlin He and Hongwei Yang \*

Synthesis of silver nanowires (Ag NWs) has been studied for decades. However, Ag NWs with diameters below 20 nm synthesised by simple and robust approaches are still rarely reported. In this work, Ag NWs with an average diameter of ~15 nm and an aspect ratio of over 1000 have been prepared by using a Grignard reagent 5-chloro-2-thienylmagnesium bromide as an assistant additive. In particular, the presence of 5-chloro-2-thienylmagnesium bromide is proven to be beneficial for the *in situ* formation of smaller AgBr and AgCl particles step by step in comparison with traditional inorganic halide ions, and then promote the final growth of ultrafine Ag NWs.

 Received 7th October 2021  
 Accepted 11th November 2021

DOI: 10.1039/d1ra07432f

[rsc.li/rsc-advances](http://rsc.li/rsc-advances)

## Introduction

The potential applications of Ag NWs in flexible electronic have attracted much attention due to their excellent electrical, optical, and mechanical properties.<sup>1–4</sup> In particular, the optical property is greatly affected by the diameter of the Ag NWs. In general, finer Ag NWs lead to lower haze and higher transmittance. To date, there are different ways to prepare Ag NWs, such as the hydrothermal method,<sup>5,6</sup> electrochemical method,<sup>7–9</sup> polyol process,<sup>10</sup> *etc.* Among these methods, the polyol process has been a much favored one. Thus far, one or more inorganic auxiliaries are usually used to prepare Ag NWs, such as NaBr, NaCl, or CuCl<sub>2</sub>, NaCl and KBr, KCl and FeCl<sub>3</sub>, *etc.* For example, Wiley *et al.* successfully synthesized Ag NWs with a diameter of ~20 nm by using NaBr as an auxiliary agent.<sup>11</sup> Zhang *et al.* reported that Ag NWs with an average diameter of 26 nm were produced through the addition of KBr to the polyol reaction medium.<sup>12</sup> Silva and co-workers reported a simple route to synthesize Ag NWs with the diameter of 20 nm and the length of approached 20 μm, in which NaBr acted as an auxiliary agent.<sup>13</sup> In another study, Ag NWs with the diameter of 20 nm could be synthesized through NaCl and KBr mediated polyol reactions by Miao *et al.*<sup>14</sup> Zhang *et al.* also investigated how the ratio of chloride to bromide influence the morphology of Ag NWs.<sup>15</sup>

In contrast, there are few literatures on the preparation of Ag NWs assisted by organic additives. For example, Zheng *et al.* successfully produced the Ag NWs with the diameter of 25 nm

by using cetyltrimethylammonium bromide and sodium dodecyl sulfate.<sup>16</sup> Yuan *et al.* prepared Ag NWs with the diameter of ~16 nm and ~20 nm by using tetrabutyl ammonium dibromochloride and 6-chlorohexylzinc bromide, respectively.<sup>17,18</sup> However, Ag NWs with the diameter below 20 nm are still seldom reported by using organic auxiliaries. It is thereby quite necessary to develop new organic auxiliaries for preparing Ag NWs with the diameter below 20 nm, which can well meet the requirement of flexible transparent conducting thin film with higher transmittance and lower haze.

Herein, 5-chloro-2-thienylmagnesium bromide is first used in place of traditional inorganic halide to prepare Ag NWs with the average diameter of 15 nm. Also, the probable controlled mechanism of 5-chloro-2-thienylmagnesium bromide in the formation of Ag NWs is discussed in detail.

## Experimental

### Materials

Poly(vinylpyrrolidone) (PVP,  $M_w \sim 1\,300\,000$ ) and ethylene glycol (EG, ≥99.0%) were obtained from Sigma Aldrich. Ethanol (C<sub>2</sub>H<sub>5</sub>OH, ≥99.0%) was purchased from Xilong Chemical Co., Ltd. Silver nitrate (AgNO<sub>3</sub>, ≥99.8%) was purchased from Sinopharm Chemical Reagent Co., Ltd. 5-Chloro-2-thienylmagnesium bromide (C<sub>4</sub>H<sub>2</sub>BrClMgS, 0.5 M solution in tetrahydrofuran, density of 0.9690) was acquired from Shanghai Aladdin industrial Co., Ltd. Deionized (DI) water, with a resistivity of not less than 18.2 MΩ cm, was prepared by a laboratory water purification system.

### Synthesis of silver nanowires

Ag NWs were synthesized by the C<sub>4</sub>H<sub>2</sub>BrClMgS-assisted polyol process. The procedure was shown as following. First, two

State Key Laboratory of Advanced Technologies for Comprehensive Utilization of Platinum Metals, Kunming Institute of Precious Metals, 650106 Kunming, People's Republic of China. E-mail: nanolab@ipm.com.cn

† Electronic supplementary information (ESI) available. See DOI: 10.1039/d1ra07432f



solutions were prepared in EG: (a) 15 mM PVP, and (b) 165 mM AgNO<sub>3</sub>. Then, 130 mL (a) and 39.5 μL C<sub>4</sub>H<sub>2</sub>BrClMgS (0.5 M solution in tetrahydrofuran) were added to a flask in order, which was placed in a water bath with constant stirring for 30 min at 298 K. After complete mixing, 20 mL (b) was added to the mixture and continued stirring for 10 min at 298 K to form a homogeneous solution. Subsequently, the solution was heated at certain temperature for 30 min. The obtained Ag NWs were collected by centrifugation of 4500 rpm for 10 min and washed thoroughly with absolute ethyl alcohol and deionized water for three times to remove the EG and PVP, and then redispersed with ethyl alcohol for further using.

### Characterizations

The microstructures of the Ag NWs were characterized by tungsten hairpin filament scanning electron microscopy (SEM, ZEISS EVO 18). High resolution transmission electron microscopy was examined on a Philips CM 200-FEG microscope (200 kV, C<sub>s</sub> = 1.35 mm), and transmission electron microscopy (TEM, Tecnai G2-TF30) was performed on the device at an accelerating voltage of 120 kV. The phase identification of the Ag NWs were performed by X-ray diffraction (XRD, Rigaku D/MAX-3B) with a Cu target and K<sub>α</sub> radiation (λ = 1.54056 Å), where the pattern was collected over the range (2θ) from 20 to 90° with a scanning step of 0.02°. UV-vis spectrophotometer (PERSEE Genera TU-1901) was used to monitor the evolution of the UV-vis spectra of the as-obtained Ag NWs.

## Results and discussion

First, we systematically investigated the effects of molar ratio of C<sub>4</sub>H<sub>2</sub>BrClMgS/AgNO<sub>3</sub> and PVP/AgNO<sub>3</sub>, and the reaction temperature on the morphology of Ag NWs. The obtained results clearly revealed that all these factors played significant roles in controlling the nanostructures of Ag NWs. Ultrafine Ag NWs could be eventually prepared at 443 K when the molar ratio of C<sub>4</sub>H<sub>2</sub>BrClMgS/AgNO<sub>3</sub> and PVP/AgNO<sub>3</sub> is 0.006 and 0.75, separately (Fig. S1–S3†). Conversely, excessive increase of C<sub>4</sub>H<sub>2</sub>BrClMgS or PVP dosage or the reaction temperature led to a mixture of Ag nanowires, nanorods and quasi-spherical nanoparticles.

In order to investigate the morphology evolution of Ag NWs during the reaction, both the time-dependent UV-vis and TEM characterizations were carried out and the results are presented in Fig. 1 and 2. When the reaction mixture was heated at 443 K for 15 min, a broad characteristic peak centered at 417 nm was monitored (Fig. 1). Meanwhile, the sample consisted of Ag nanoparticles with the size range of 5–50 nm could be observed in Fig. 2a. It is noted that these Ag nanoparticles resemble the decahedral multiply twinned seed towards Ag NWs with a penta-twinned structure.<sup>19</sup> Subsequently, the characteristic peak at 417 nm decline and a new extinction peak at 370 nm appears, together with a shoulder at 358 nm as the reaction was extended to 20 min. The peak at 370 nm can be attributed to the transverse localized surface plasmon

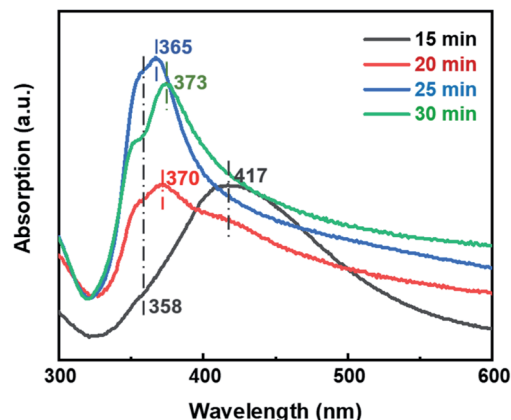


Fig. 1 UV-vis spectra of products prepared at different stages. The molar ratio of C<sub>4</sub>H<sub>2</sub>BrClMgS/AgNO<sub>3</sub> and PVP/AgNO<sub>3</sub> is 0.006 and 0.75, and the reaction temperature is at 443 K.

resonance (LSPR) mode of one-dimensional silver nanostructures, indicating that more Ag nanorods and nanowires were produced.<sup>11,20</sup> As shown in Fig. 2b, Ag nanorods with the length range of 100–300 nm and the diameter below 20 nm indeed formed in the reaction solution. When extending the reaction to 25 min, the transverse LSPR peak of the Ag nanowires slightly blue-shifts to 365 nm, implying the formation of Ag NWs with thinner diameter.<sup>21</sup> At this point, the average

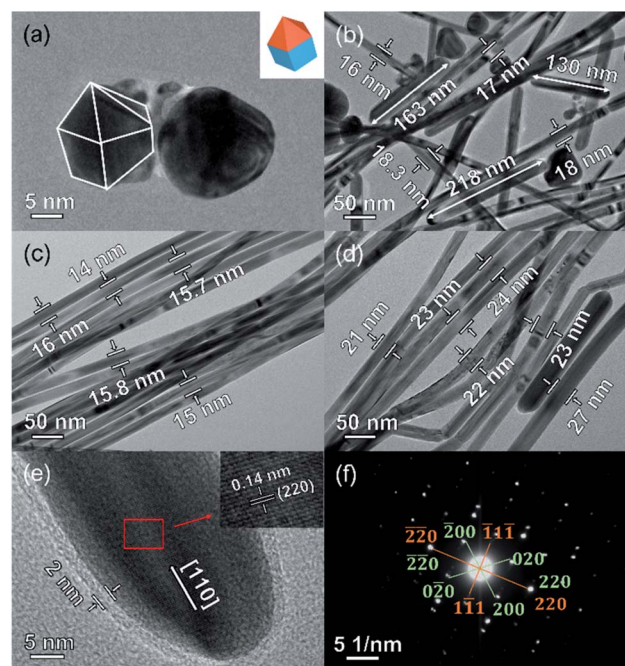


Fig. 2 TEM images of products prepared at different stages: (a) 15 min, (b) 20 min, (c) 25 min, (d) 30 min, (e) HRTEM image of single Ag NW, (f) SAED pattern corresponds to a superposition of [001] (marked in green) and [111] (marked in orange) zone patterns of fcc Ag with the double-diffraction reflections. The molar ratio of C<sub>4</sub>H<sub>2</sub>BrClMgS/AgNO<sub>3</sub> and PVP/AgNO<sub>3</sub> is 0.006 and 0.75, and the reaction temperature is at 443 K.



diameter of the Ag NWs was decreased to 15 nm, as TEM results showed in Fig. 2c. Further prolonging the reaction time up to 30 min, a characteristic peak around 373 nm can be observed, owing to the lateral plasmon resonance absorption that evidently red-shifts to the high wavelength position. Accordingly, the TEM image of sample obtained reveals that the average diameter of Ag NWs is increased to 24 nm (Fig. 2d). In particular, the HRTEM image in Fig. 2e shows that the Ag NWs obtained have a 2 nm thick PVP capping agent and the lattice structure appears clearly with a lattice distance of 0.14 nm, which is in agreement with the values for the (220) planes of face-centered cubic (fcc) Ag.<sup>22</sup> Fig. 2f presents the selected-area electron diffraction (SAED) patterns along the  $[\bar{1}12]$  and  $[001]$  crystallographic zone axes. It is clear that the obtained Ag NWs possess a twin crystalline structure. Therefore, the ultrafine Ag NWs synthesized in this work should have a penta-twined structure and are bounded by five  $\{100\}$  side faces and ten  $\{111\}$  end faces.<sup>19,23</sup>

SEM images of Ag NWs before and after purification further display that the original Ag NWs contain some nanoparticles, while cleaned Ag NWs with the length over 15  $\mu\text{m}$  are obtained after centrifugation treatment (Fig. 3a and b). Accordingly, it is obvious that the transverse LSPR peak of the purified Ag NWs slightly blue-shifts to 363 nm, while the band from 400 nm to 600 nm distinctly declines, implying that the Ag nanoparticles have been almost removed (Fig. 3c).<sup>24</sup>

The XRD characterization was conducted to elucidate the crystalline nature of the ultrafine Ag NWs, as shown in Fig. 4. The results indicate that the crystal structure of Ag NWs is the face-centered cubic (fcc) structure by comparing the dotted line with JCPDS (No. 04-0783) of Ag. The apparent five peaks at  $38.1^\circ$ ,  $44.3^\circ$ ,  $64.4^\circ$ ,  $77.4^\circ$ , and  $81.5^\circ$  correspond to the (111), (200), (220), (311), and (222) Bragg reflections of silver. However, the peak positions are slightly shifted from the

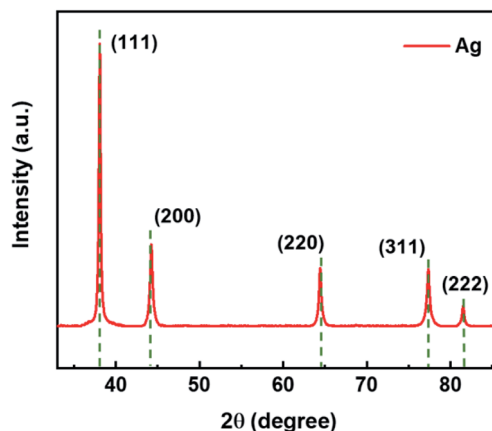


Fig. 4 XRD pattern of Ag NWs. The molar ratio of  $\text{C}_4\text{H}_2\text{BrClMgS}/\text{AgNO}_3$  and  $\text{PVP}/\text{AgNO}_3$  is 0.006 and 0.75, and the reaction temperature is at 443 K.

values of perfect fcc silver (dashed vertical lines), which should be the consequence of the lattice strain in the nanowires. As previously reported, the tensile strain of the (220) crystal planes and the compressive strain of the (200) crystal planes, the corresponding peaks will move to smaller and larger  $2\theta$ -values, respectively.<sup>25</sup> Additionally, it can be noted that the intensity ratios of the (111) and (200) peaks are relatively high, implying that the Ag NWs grow along the  $[110]$  direction.<sup>18,26</sup>

Based upon the above results and discussions, a possible growth mechanism of Ag NWs is proposed. As revealed in Scheme 1, AgBr and AgCl will successively form *via* the chemical reaction (1)–(3) as increasing the reaction temperature.<sup>27</sup> In contrast to the traditional inorganic halide ions, this unique process may promote the slow production of AgBr and AgCl particles in the reaction solution. The subsequent SEM and EDS results further indicate that the Grignard reagent  $\text{C}_4\text{H}_2\text{BrClMgS}$  is indeed beneficial for the formation of smaller AgBr and AgCl seeds (Fig. S4 and S5<sup>†</sup>), on which ultrafine Ag NWs can grow *in situ*.<sup>15,17</sup> When using NaBr and NaCl (the molar ratio of  $\text{Br}^-/\text{AgNO}_3$  and  $\text{Cl}^-/\text{AgNO}_3$  are equal to the molar ratio of  $\text{C}_4\text{H}_2\text{BrClMgS}/\text{AgNO}_3$ ) as the dual additives in the controlled experiment, the diameter of Ag NWs and Ag nanorods obtained was in the range of 30–100 nm. Simultaneously, the original product contained lots of nanoparticles and nanorods besides few nanowires (Fig. S6<sup>†</sup>).

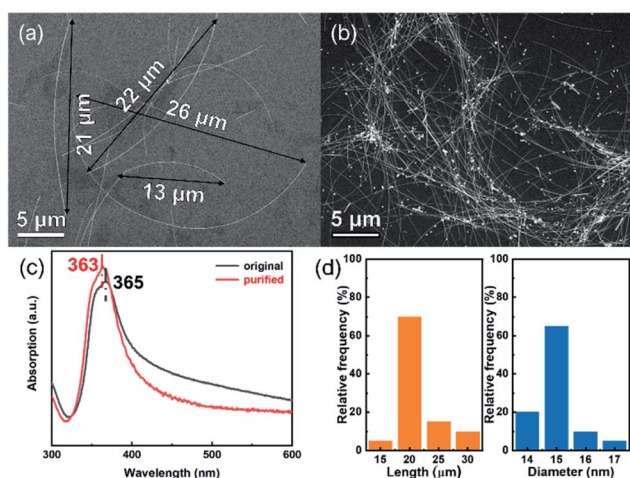
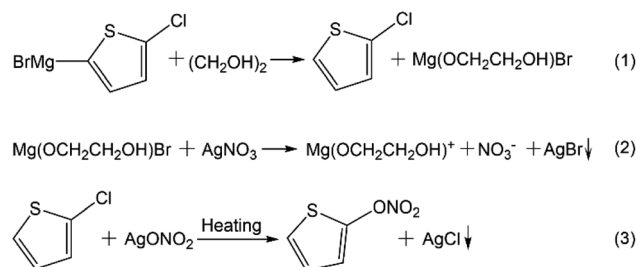


Fig. 3 SEM images of Ag NWs before and after purification: (a) the purified products, (b) the original products, (c) UV-vis spectra of Ag NWs before and after purification. (d) Histogram of statistics about length and diameter of Ag NWs. The molar ratio of  $\text{C}_4\text{H}_2\text{BrClMgS}/\text{AgNO}_3$  and  $\text{PVP}/\text{AgNO}_3$  is 0.006 and 0.75, and the reaction temperature is at 443 K.



Scheme 1 Chemical equations of reaction process.





## Conclusions

In summary, this work demonstrates that Ag NWs with the average diameter down to 15 nm and the average length of over 15  $\mu\text{m}$  can be synthesized by using  $\text{C}_4\text{H}_2\text{BrClMgS}$  as the organic auxiliary. This novel Grignard reagent has been verified to prompt the production of AgBr and AgCl particles step by step, which is favorable for the formation of smaller AgCl and AgBr seeds, and eventually leading to the *in situ* growth of ultrafine Ag NWs on these seeds surface.

## Conflicts of interest

The authors declare that they have no known competing financial interests or personal relationships that could have appeared to influence the work reported in this paper.

## Acknowledgements

This work was supported by Major R&D Project of Yunnan Province (Grant No. 202002AB080001-1, 202102AB080008), National Natural Science Foundation of China (Grant No. 21761016), Young and Middle aged Academic and Technical Leaders Reserve Talents Program of Yunnan Province (Grant No. 2017HB060), and Ten Thousand Talents Plan-Young Top Talent Program of Yunnan Province.

## References

- Z. Yu, Q. Zhang, L. Li, Q. Chen, X. Niu, J. Liu and Q. Pei, *Adv. Mater.*, 2011, **23**, 664–668.
- M. Amjadi, A. Pichitpajongkit, S. Lee, S. Ryu and I. Park, *ACS Nano*, 2014, **8**, 5154–5163.
- M.-X. Jing, M. Li, C.-Y. Chen, Z. Wang and X.-Q. Shen, *J. Mater. Sci.*, 2015, **50**, 6437–6443.
- D. J. Lee, Y. Oh, J.-M. Hong, Y. W. Park and B.-K. Ju, *Sci. Rep.*, 2018, **8**, 1–9.
- Y. Li, S. Guo, H. Yang, Y. Chao, S. Jiang and C. Wang, *RSC Adv.*, 2018, **8**, 8057–8063.
- J. Xu, J. Hu, C. Peng, H. Liu and Y. Hu, *J. Colloid Interface Sci.*, 2006, **298**, 689–693.
- X. J. Xu, G. T. Fei, X. W. Wang, Z. Jin, W. H. Yu and L. De Zhang, *Mater. Lett.*, 2007, **61**, 19–22.
- M. Fu, L. Qian, H. Long, K. Wang, P. Lu, Y. P. Rakovich, F. Hetsch, A. S. Susha and A. L. Rogach, *Nanoscale*, 2014, **6**, 9192–9197.
- S. Yin, D. Zhao, Q. Ji, Y. Xia, S. Xia, X. Wang, M. Wang, J. Ban, Y. Zhang and E. Metwalli, *ACS Nano*, 2018, **12**, 861–875.
- Y. Li, Y. Li, Z. Fan, H. Yang, X. Yuan and C. Wang, *RSC Adv.*, 2020, **10**, 21369–21374.
- B. Li, S. Ye, I. E. Stewart, S. Alvarez and B. J. Wiley, *Nano Lett.*, 2015, **15**, 6722–6726.
- K. Zhang, Y. Du and S. Chen, *Org. Electron.*, 2015, **26**, 380–385.
- R. R. Da Silva, M. Yang, S.-I. Choi, M. Chi, M. Luo, C. Zhang, Z.-Y. Li, P. H. Camargo, S. J. L. Ribeiro and Y. Xia, *ACS Nano*, 2016, **10**, 7892–7900.
- J. Miao, S. Chen, H. Liu and X. Zhang, *Chem. Eng. J.*, 2018, **345**, 260–270.
- P. Zhang, Y. Wei, M. Ou, Z. Huang, S. Lin, Y. Tu and J. Hu, *Mater. Lett.*, 2018, **213**, 23–26.
- X. Zheng, L. Zhu, A. Yan, X. Wang and Y. Xie, *J. Colloid Interface Sci.*, 2003, **268**, 357–361.
- X. Yuan, H. Yang, Y. Li, Y. Li, Y. Chao, J. Chen and L. Chen, *Langmuir*, 2019, **35**, 11829–11835.
- X. Yuan, H. Yang, Y. Li, Y. Chao, Y. Li, L. Chen and J. Chen, *RSC Adv.*, 2019, **9**, 18868–18873.
- Y. Sun, B. Mayers, T. Herricks and Y. Xia, *Nano Lett.*, 2003, **3**, 955–960.
- K. L. Kelly, E. Coronado, L. L. Zhao and G. C. Schatz, *J. Phys. Chem. B*, 2003, **3**, 668–677.
- Y. Sun, B. Gates, B. Mayers and Y. Xia, *Nano Lett.*, 2002, **2**, 165–168.
- E. Ringe, R. P. Van Duyne and L. D. Marks, *J. Phys. Chem. C*, 2013, **117**, 15859–15870.
- F. Xu, H. Hou and Z. Gao, *ChemPhysChem*, 2014, **15**, 3979–3986.
- H.-W. Jang, Y.-H. Kim, K.-W. Lee, Y.-M. Kim and J.-Y. Kim, *APL Mater.*, 2017, **5**, 080701–080707.
- F. Niekel, E. Bitzek and E. Spiecker, *ACS Nano*, 2014, **8**, 1629–1638.
- J. P. Kottmann, O. J. Martin, D. R. Smith and S. Schultz, *Phys. Rev. B: Condens. Matter Mater. Phys.*, 2001, **64**, 235402–235411.
- J. McMurry, Alkyl Halides, in *Fundamentals of Organic Chemistry*, Thomson-Brooks/Cole, 5th edn, 2003, pp. 211–242.

